

Ratio of J/ψ production cross sections in deep inelastic muon scattering from tin and carbon

THE NEW MUON COLLABORATION (NMC)

P. Amaudruz ^{a,1}, M. Arneodo ^b, A. Arvidson ^c, B. Badelek ^d, G. Baum ^e,
J. Beaufays ^{f,2}, I.G. Bird ^{g,3}, M. Botje ^a, C. Brogini ^{h,4}, W. Brückner ^g, A. Brüll ⁱ,
W.J. Burger ^{a,5}, J. Ciborowski ^d, R. van Dantzig ^f, H. Döbbling ^{g,6}, J. Domingo ^{a,7},
J. Drinkard ^j, M. Düren ^g, H. Engelen ⁱ, M.I. Ferrero ^b, L. Fluri ^h,
D. von Harrach ^{g,8}, M. van der Heijden ^f, C. Heusch ^j, Q. Ingram ^a, K. Janson ^c,
M. de Jong ^f, E.M. Kabuss ^{g,8}, R. Kaiser ⁱ, T.J. Ketel ^f, F. Klein ^k, S. Kullander ^c,
U. Landgraf ⁱ, T. Lindqvist ^c, G.K. Mallot ^k, C. Mariotti ^b, G. van Middelkoop ^{l,f},
Y. Mizuno ^{g,9}, J. Nassalski ^m, D. Nowotny ^{g,10}, C. Peroni ^b, B. Povh ^{g,n},
R. Rieger ^k, K. Rith ^g, K. Röhrich ^{k,11}, E. Rondio ^d, L. Ropelewski ^d,
A. Sandacz ^m, C. Scholz ^g, U. Sennhauser ^{a,12}, F. Sever ^{e,13}, T.-A. Shibata ⁿ,
M. Siebler ^e, A. Simon ^g, A. Staiano ^b, Y. Tzamouranis ^{g,14},
J.L. Vuilleumier ^h, T. Walcher ^k, R. Windmolders ^o and F. Zetsche ^g

^a Paul Scherrer Institut, CH-5234 Villigen, Switzerland

^b Università di Torino and INFN, I-10125 Turin, Italy

^c University of Uppsala, S-75121 Uppsala, Sweden

^d University of Warsaw, PL-00-681 Warsaw, Poland ¹⁵

^e Universität Bielefeld, W-4800 Bielefeld, Germany ¹⁶

¹ Present address: TRIUMF, Vancouver, BC V6T 2A3, Canada.

² Present address: Trasys, 1930 Zaventem, Belgium.

³ Present address: NIKHEF-K, P.O. Box 4395, 1009 AJ Amsterdam, The Netherlands.

⁴ Present address: INFN, Laboratori Nazionali del Gran Sasso, 67010 Assergi, Italy.

⁵ Present address: Université de Genève, 1211 Genève 4, Switzerland.

⁶ Present address: GSI, W-6100 Darmstadt, Germany.

⁷ Present address: CEBAF, Newport News, VA 23606, USA.

⁸ Present address: University of Mainz, W-6500 Mainz, Germany.

⁹ Present address: Osaka University, 567 Osaka, Japan.

¹⁰ Present address: SAP AG, W-6909 Walldorf, Germany.

¹¹ Present address: IKP2-KFA, W-5170 Jülich, Germany.

¹² Present address: EMPA, 8600 Dübendorf, Switzerland.

¹³ On leave from Jozef Stefan Institut, Ljubljana, Yugoslavia, present address: DPhN Saclay, 91191 Gif-sur-Yvette, France.

¹⁴ Present address: University of Houston, TX 77204-5504, USA.

¹⁵ Supported by CPBP.01.09.

¹⁶ Supported by Bundesministerium für Forschung und Technologie.

^f NIKHEF-K, NL-1009 AJ Amsterdam, The Netherlands ¹⁷

^g Max-Planck Institut, W-6900 Heidelberg, Germany ¹⁶

^h Université de Neuchâtel, CH-2000 Neuchâtel, Switzerland

ⁱ Universität Freiburg, W-7800 Freiburg, Germany ¹⁶

^j University of California, Santa Cruz, CA 95064, USA

^k Universität Mainz, W-6500 Mainz, Germany ¹⁶

^l CERN, CH-1211 Geneva 23, Switzerland

^m Institute for Nuclear Studies, PL-00-681 Warsaw, Poland ¹⁸

ⁿ Universität Heidelberg, W-6900 Heidelberg, Germany ¹⁶

^o Université de L'Etat Mons, B-7000, Belgium

Received 11 November 1991

Accepted for publication 26 November 1991

We present results on J/ψ production in muon interactions with tin and carbon targets at incident muon energies of 200 and 280 GeV. The ratio of cross sections per nucleon for J/ψ production on tin and carbon, $R(\text{Sn}/\text{C})$, is studied as a function of p_T^2 , z and x . We find an enhancement for coherent J/ψ production $R_{\text{coh}}(\text{Sn}/\text{C}) = 1.54 \pm 0.07$, a suppression for quasielastic production $R_{\text{qe}}(\text{Sn}/\text{C}) = 0.79 \pm 0.06$ and for inelastic production $R_{\text{in}}(\text{Sn}/\text{C}) = 1.13 \pm 0.08$. The inelastic cross section ratio can be interpreted within the Colour Singlet model as an enhancement of the gluon distribution in tin with respect to that in carbon. The dependence of the ratio on z and p_T^2 can explain the discrepancy between the results obtained in previous experiments.

1. Introduction

The discovery of the EMC effect [1], that the structure function F_2 of a nucleon bound in a nucleus is different from that of a free nucleon, has stimulated a wide range of experimental [2,3] and theoretical activities [4]. It is important to determine whether such an effect also manifests itself in the gluon momentum distribution in the nucleon. This can be investigated by studying the production of the J/ψ particle in deep inelastic scattering [5].

In the kinematic region where the J/ψ is produced inelastically and incoherently (later referred to as inelastic) the virtual photon couples to the constituents of the nucleon. The Colour Singlet (CS) model [5] was found to give a good description of this production mechanism [6–9]. Within this model the inelastic cross section is proportional to the gluon momentum distribution so that the ratio of gluon distributions for different nuclei can be obtained from the cross section ratio.

In the process of J/ψ production in muon interactions with nuclei other contributions are present. The production cross section can be considered as the sum of the cross sections for coherent, quasielastic and inelastic interactions. In coherent J/ψ production the recoiling nucleus emerges intact from the interaction, whereas in quasielastic production the interaction occurs elastically with a

¹⁷ Supported in part by FOM, Vrije Universiteit Amsterdam and NWO.

¹⁸ Supported by CPBP.01.06.

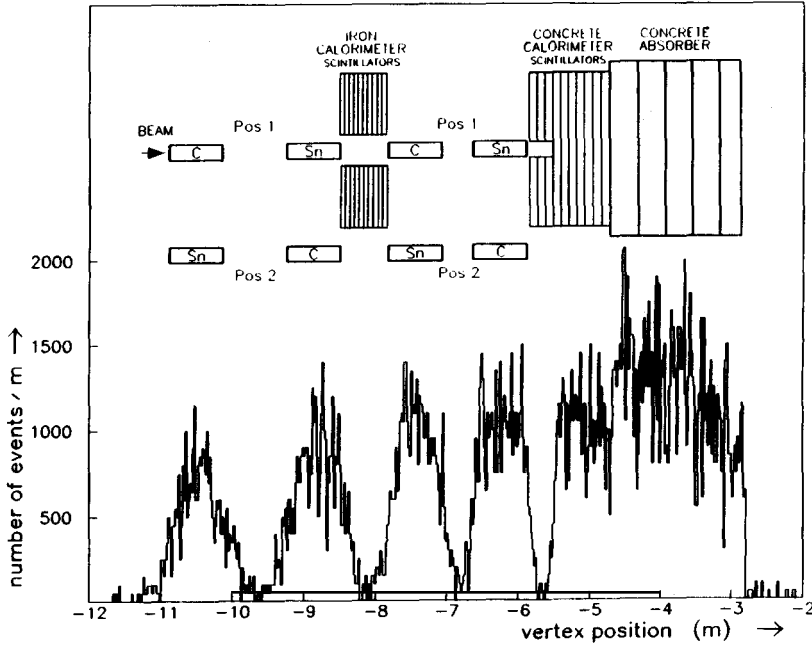


Fig. 1. The target set-up and the distribution of the reconstructed vertex positions along the beam direction summed over both target positions.

nucleon in the nucleus. We separated the kinematic regions where each of the above mentioned mechanisms is dominant to provide information on each of these processes. Since the mechanisms are different, one may expect the corresponding cross section ratios for heavy and light nuclei to be different. In the present paper we show that the seemingly inconsistent results obtained over the past fifteen years for such ratios can be reconciled.

2. Experiment and analysis

The experiment was performed at the M2 muon beam line of the CERN SPS with a modified and upgraded version of the EMC forward spectrometer [10]. The data presented here were collected at two incident energies, 200 and 280 GeV.

A complementary target set-up was used, allowing measurements of cross section ratios of different target materials with small systematic errors. Each target set consisted of two tin and two carbon targets in alternate order. The complementary sets (see fig. 1), where carbon and tin were interchanged, were alternately exposed to the beam. The tin targets were segmented such that the extent and the total amount of material along the beam were the same as for the carbon targets. Each target had a thickness of approximately 150 g/cm^2 . Acceptances and inte-

grated beam fluxes cancel in the calculation of the cross section ratio. The frequent exchange of the target sets also minimises the effects of any time dependence in the apparatus acceptance. A passive concrete absorber shielded the spectrometer from the electromagnetic and hadronic cascades originating from the interaction vertex. Data were collected using a specially designed trigger [8] which selected multimMuon tracks originating from the target. The information from the target calorimeters was not used.

The kinematics of the reaction was reconstructed from the measured momenta of both J/ψ decay muons together with the incident and scattered muon. A special algorithm was devised to reconstruct tracks of particles scattered at very small angles and thus remaining in the beam region. Events with three or more outgoing muon tracks were selected for the analysis. For each event the hardware trigger requirements were checked using the reconstructed muon trajectories. To select the J/ψ decay muons, the invariant mass of pairs of oppositely charged particles was calculated for the selected data sample. The track pair with an invariant mass closest to the J/ψ rest mass was then taken. The scattered muon was selected from the other reconstructed tracks requiring the same charge as the incident muon. In 9% of the selected events more than one candidate for the scattered muon was found. These events were subjected to a further selection procedure in which the muon with the highest energy was chosen whenever its energy was at least 50% higher than the energy of any other candidate. Otherwise, the track with the smallest scattering angle was taken [7]. The kinematic variables used in the present analysis are listed in table 1. Cuts are applied in order to exclude regions of poor acceptance and high background contamination. These cuts are listed in table 2 for the two data samples.

Fig. 1 shows the distribution of the reconstructed vertex positions along the beam direction. The vertex resolution was good enough to distinguish between the targets. The probability of associating events to the wrong material was found to be less than 1%.

TABLE 1
Kinematic variables

| Variable | Description |
|-----------------------------|--|
| $k = (E, \mathbf{k})$ | 4-momentum of the incident muon |
| $k' = (E', \mathbf{k}')$ | 4-momentum of the scattered muon |
| $q = k - k'$ | 4-momentum of the virtual photon |
| $q^2 = -Q^2$ | invariant mass squared of the virtual photon |
| $\nu = E - E'$ | energy of the virtual photon in the laboratory frame |
| $s = M_N^2 + 2M_N\nu - Q^2$ | the square of the photon-nucleon centre-of-mass energy |
| $z = E_{J/\psi} / \nu$ | energy fraction carried by the J/ψ in the laboratory frame |
| p_T^2 | transverse momentum squared of the J/ψ with respect to the photon direction |
| θ_{decay} | the angle of the positive decay muon in the helicity frame |

TABLE 2
Cuts applied in the event selection

| Variable | Lower Limit | Upper Limit | Units |
|-------------------------------|-------------|-------------|--------------------|
| E'_μ | 15 | | GeV |
| $E_{\text{decay } \mu}$ | 10 | | GeV |
| $\nu(E = 200 \text{ GeV})$ | 40 | 180 | GeV |
| $\nu(E = 280 \text{ GeV})$ | 60 | 240 | GeV |
| Q^2 | | 20 | GeV^2 |
| p_T^2 | | 10 | $(\text{GeV}/c)^2$ |
| z | 0.2 | 1.1 | |
| $\cos(\theta_{\text{decay}})$ | -0.9 | 0.9 | |
| $M_{\mu^+\mu^-}$ | 2.7 | 3.5 | GeV/c^2 |

Fig. 2 shows the distribution of the invariant mass $M_{\mu^+\mu^-}$ of the selected muon pairs for tin and carbon for the 280 GeV data sample. The sum of a gaussian distribution and an exponentially falling background was fitted to each of the mass spectra (smooth curves in the figure). Subtracting the fitted background from the number of events in the mass interval $2.7 \text{ GeV}/c^2 \leq M_{\mu^+\mu^-} \leq 3.5 \text{ GeV}/c^2$, the final J/ψ yields were found to be 514 ± 30 (Sn) and 416 ± 24 (C) events at 200 GeV and 1353 ± 46 (Sn) and 1137 ± 40 (C) events at 280 GeV. The fitted values of the peak positions are in agreement with the known value of the J/ψ rest mass [11] (see table 3). The widths of the gaussian distributions are determined by the experimental momentum resolution and by multiple scattering in the targets and concrete absorber. This was verified by Monte Carlo studies.

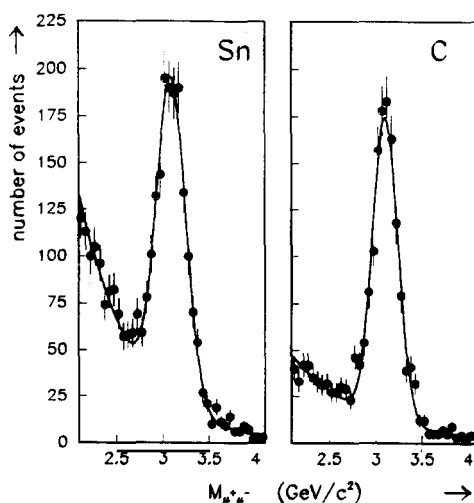


Fig. 2. Invariant mass distributions of selected $\mu^+\mu^-$ pairs from tin and carbon at 280 GeV incident muon energy. The smooth curves are fits to the observed distributions (see text).

TABLE 3
Results of the fits of the function $a e^{-(M_{\mu^+\mu^-}-M_0)^2/2\sigma^2} + b e^{-cM_{\mu^+\mu^-}}$ to the mass spectra

| Target | E (GeV) | M_0 (MeV/ c^2) | σ (MeV/ c^2) |
|--------|-----------|---------------------|------------------------|
| C | 200 | 3090 ± 8 | 144 ± 8 |
| Sn | 200 | 3095 ± 8 | 136 ± 9 |
| C | 280 | 3104 ± 5 | 137 ± 5 |
| Sn | 280 | 3092 ± 6 | 156 ± 5 |

A signal of ψ' production is visible in the mass spectrum of muon pairs from events originating in the passive absorber at 280 GeV (see fig. 3). For these events the mass resolution is better because of the reduced multiple scattering. Two gaussian distributions on top of an exponentially falling background were fitted simultaneously to the mass spectrum (smooth curve in the figure). Subtracting the fitted background from the number of events in the mass intervals $2.8 \text{ GeV}/c^2 \leq M_{\mu^+\mu^-} \leq 3.4 \text{ GeV}/c^2$ and $3.4 \text{ GeV}/c^2 \leq M_{\mu^+\mu^-} \leq 3.9 \text{ GeV}/c^2$, the final J/ψ and ψ' yields are 2415 ± 58 and 53 ± 14 events, respectively. After dividing these yields by the corresponding branching ratios $\text{BR}(J/\psi \rightarrow \mu^+\mu^-) = 6.9 \pm 0.9\%$ and $\text{BR}(\psi' \rightarrow \mu^+\mu^-) = 0.77 \pm 0.17\%$ [11], one obtains the cross section ratio $\sigma(\psi')/\sigma(J/\psi) = 0.20 \pm 0.05(\text{stat.}) \pm 0.07(\text{syst.})$. The systematic error arises from the uncertainty in the branching ratios. The present result compares well with the value of ref. [12].

It was found earlier that the cross section per nucleon in deuterium is equal to that in hydrogen: $\sigma^N(\text{D})/\sigma^N(\text{H}) = 0.96 \pm 0.08$ [8]. The tin to carbon cross section

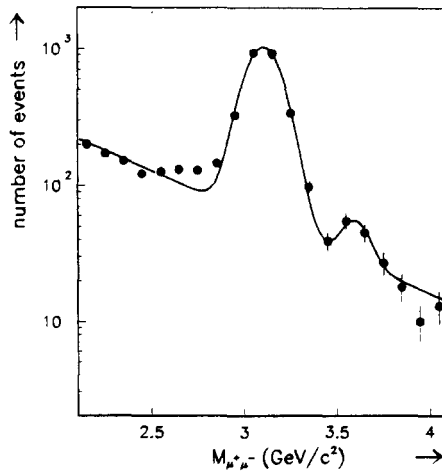


Fig. 3. Invariant mass distribution of selected $\mu^+\mu^-$ pairs from the concrete absorber at 280 GeV incident muon energy. The smooth curve is discussed in the text.

ratio was therefore not corrected for the non-isoscalarity of the tin target, since such a correction would be less than 1%.

3. Ratio of J/ψ production cross sections

3.1. COHERENT J/ψ PRODUCTION

In coherent J/ψ production the recoiling nucleus emerges intact from the interaction. Since the nucleus carries away little energy most of the energy of the photon is transferred to the J/ψ , so that the energy fraction z is close to unity.

Coherent photoproduction of vector mesons is usually interpreted in terms of Vector Meson Dominance (VMD) [13]. In the application of the VMD model to muoproduction of J/ψ mesons it is assumed that the virtual photon couples to an off-shell J/ψ meson which is put on-shell by diffractive scattering from a target nucleus. The total nuclear cross section for coherent production is usually taken to be of the form [13]

$$\sigma_{\text{coh}}(\gamma^*A) = \left(\frac{d\sigma(\gamma^*p)}{dt} \right)_{t=0} A^2 \int_{t_{\min}}^{t_{\max}} F^2(-t) dt, \quad (1)$$

where $t = (q - p_{J/\psi})^2$ with $p_{J/\psi}$ the four-momentum of the J/ψ , $t_{\min} = -((Q^2 + M_{J/\psi}^2)/2\nu)^2$ at $z = 1$, t_{\max} is determined by the applied cuts, A is the atomic number and $F(-t)$ is the form factor of the nucleus.

The calculation of t involves the subtraction of two measured quantities of similar size. Consequently the resolution in t is poor especially at small t and the coherent peak arising from the form factor cannot be resolved. Since p_{T}^2 is measured much more accurately and $p_{\text{T}}^2 \approx |t - t_{\min}|$ for z close to unity, the p_{T}^2 distribution is used to study the coherent peak. Fig. 4 shows the p_{T}^2 distributions for carbon and tin at 200 and 280 GeV in the high- z region ($z \geq 0.9$). The curves are fits to the four data-sets with the sum of two exponentials

$$f(p_{\text{T}}^2) = a_1 e^{-b_1 p_{\text{T}}^2} + a_2 e^{-b_2 p_{\text{T}}^2}. \quad (2)$$

The first term describes the low- p_{T}^2 region where coherent production dominates and the second term the high- p_{T}^2 region where the J/ψ mesons are produced quasielastically. The results of the fits are given in table 4. The peaks at small p_{T}^2 , arising from coherent scattering from nuclei, are smeared by multiple scattering. The experimental p_{T}^2 resolution of $0.07 \text{ (GeV}/c)^2$ does not allow a measurement of the intrinsic shapes of the C and Sn coherent peaks.

In order to obtain information on the coherent process, $p_{\text{T}}^2 \leq 0.3 \text{ (GeV}/c)^2$ was required for the high- z data ($z \geq 0.9$). The quasielastic contribution in this region

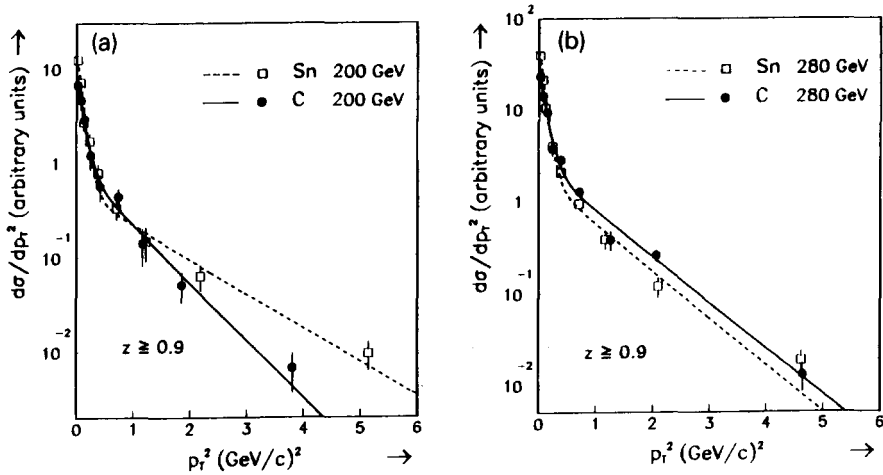


Fig. 4. The p_T^2 distributions of the high- z ($z \geq 0.9$) J/ψ signal for carbon and tin at 200 and 280 GeV incident muon energies. The solid (dashed) curves are fits of eq. (2) to the observed distributions of C (Sn).

TABLE 4
Results of the fits of the function $a_1 e^{-b_1 p_T^2} + a_2 e^{-b_2 p_T^2}$ to the p_T^2 distributions of elastic J/ψ production

| Target | E (GeV) | a_1 | b_1 (GeV/c) $^{-2}$ | a_2 | b_2 (GeV/c) $^{-2}$ |
|--------|-----------|----------------|-----------------------|-----------------|-----------------------|
| C | 200 | 7.4 ± 1.3 | 9.4 ± 1.9 | 0.88 ± 0.36 | 1.40 ± 0.24 |
| Sn | 200 | 14.2 ± 2.3 | 11.2 ± 1.8 | 0.50 ± 0.15 | 0.83 ± 0.14 |
| C | 280 | 23.9 ± 2.8 | 8.9 ± 1.2 | 2.47 ± 0.41 | 1.15 ± 0.09 |
| Sn | 280 | 45.9 ± 4.2 | 11.5 ± 1.0 | 1.86 ± 0.44 | 1.18 ± 0.17 |

is given by the fit (second term in eq. (2)) corrected by the suppression factor due to the Pauli exclusion principle [14]. This contribution affects the ratio by 3% and 10% for the 200 and 280 GeV data, respectively. The ratios obtained for the

TABLE 5
Ratio $R(\text{Sn}/\text{C})$ of the cross sections per nucleon for J/ψ production in the different kinematic regions

| | 200 GeV | 280 GeV | Combined |
|--|-----------------|-----------------|-----------------|
| Coherent events | | | |
| $z \geq 0.9, p_T^2 \leq 0.3$ (GeV/c) 2 | 1.43 ± 0.14 | 1.58 ± 0.08 | 1.54 ± 0.07 |
| Quasielastic events | | | |
| $z \geq 0.9, p_T^2 \geq 0.4$ (GeV/c) 2 | 0.94 ± 0.14 | 0.73 ± 0.07 | 0.79 ± 0.06 |
| Inelastic events | | | |
| $z \leq 0.85, p_T^2 \geq 0.4$ (GeV/c) 2 | 1.10 ± 0.18 | 1.14 ± 0.10 | 1.13 ± 0.08 |

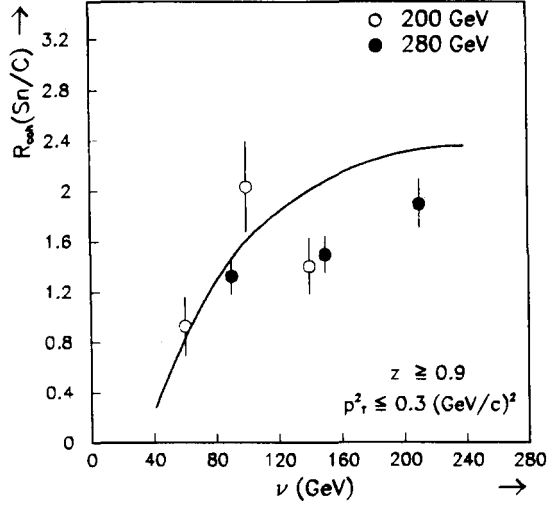


Fig. 5. Ratio of coherent J/ψ production cross sections per nucleon $R_{\text{coh}}(\text{Sn}/\text{C})$ as a function of ν , for 200 and 280 GeV incident muon energies. The curve is discussed in the text.

coherent cross sections per nucleon $R_{\text{coh}}(\text{Sn}/\text{C})$ are given in table 5, and are shown in fig. 5 as a function of ν . The curve represents the function

$$A_{\text{Sn}} \int_{t_{\text{min}}}^{t_{\text{max}}} F_{\text{Sn}}^2(-t) dt / A_{\text{C}} \int_{t_{\text{min}}}^{t_{\text{max}}} F_{\text{C}}^2(-t) dt, \quad (3)$$

where the nuclear form-factors $F_{\text{Sn}}(-t)$ and $F_{\text{C}}(-t)$ are taken from ref. [15]. Absorption effects of the J/ψ are ignored. The ratio increases with ν since the value of $|t_{\text{min}}|$ decreases with ν . A similar dependence can be seen in the data.

3.2. INELASTIC AND QUASIELASTIC J/ψ PRODUCTION

Within the framework of the Colour Singlet model [5-9,16] it is possible to extract the gluon momentum distribution $G(x)$ from the cross section for inelastic J/ψ production. By measuring the cross section ratio of inelastic J/ψ production from Sn and C it is then possible to obtain information on the ratio $G_{\text{Sn}}(x)/G_{\text{C}}(x)$ since the cross section is proportional to $G(x)$. The parameters of the model, the strong coupling constant α_s , the J/ψ leptonic width $\Gamma_{\mu^+\mu^-}$ and the charmed quark mass m_c cancel in this ratio. In order to apply the CS model in the region of its validity it is important to isolate a well defined sample of inelastic events according to z and p_T^2 .

Although the quasielastic events occur at z near unity, the experimental resolution in z is such that $z \leq 0.85$ is required to safely exclude the elastic contribution. This value was determined from Monte Carlo studies. The p_T^2

function of x is shown in fig. 8. The variable x is the fraction of the nucleon momentum carried by the gluon and it is defined as [5,16]

$$x = \frac{1}{s} \left(\frac{M_{J/\psi}^2}{z} + \frac{p_T^2}{z(1-z)} \right). \quad (4)$$

Contamination from quasielastic ψ' production and subsequent decay into J/ψ would increase the ratio $R_{\text{in}}(\text{Sn}/\text{C})$ under the assumption that the ratio for quasielastic ψ' production cross sections is the same as that for the J/ψ .

Different models [17–19] which describe shadowing in the nucleon structure function F_2 give predictions for the ratio of gluon distributions $G_A(x)/G_D(x)$. The common feature of these models is an enhancement by 3–8% of the gluon momentum distributions in the x region covered by the present data [0.02, 0.2].

4. Comparison with previous experiments

The production of J/ψ mesons has been previously studied with real and virtual photons both on hydrogen and on nuclear targets. At SLAC [20] J/ψ production was measured on Be and Ta with real photons of 20 GeV and the quasielastic cross section ratio was extracted. Another real-photon experiment ($E_\gamma = 80\text{--}190$ GeV) was performed at FNAL on several nuclei [21]. The energy fraction z was not measured and coherent effects were corrected for only by excluding events with $p_T^2 \leq 0.15$ (GeV/c)². The only previous virtual-photon experiments on different targets were performed at CERN by the EMC [22], which measured J/ψ muoproduction on H and D (at 280 GeV incident energy) and Fe (at 250 GeV incident energy). Cross sections were obtained over the full z and p_T^2 ranges, with a correction for coherence in Fe in the region $z \geq 0.95$ and $p_T^2 \leq 0.18$ (GeV/c)².

The present results, which were obtained in well defined kinematic regions, can now be compared with those obtained earlier although not always under identical conditions. The quasielastic ratio $R_{\text{qe}}(\text{Ta}/\text{Be}) = 0.83 \pm 0.05$ obtained at SLAC can be compared with the present value (0.79 ± 0.06) for Sn/C at much higher photon-energies. The production cross section ratio corrected for coherence effects as found at FNAL, $R(\text{Fe}/\text{Be}) = 0.79 \pm 0.08$, can be reproduced from the present data by restricting p_T^2 to values larger than 0.4 (GeV/c)² to exclude coherence and by integrating over the z -range accessible to our experiment [0.2, 1.1]. By requiring the same energy domain, i.e. $80 \text{ GeV} \leq \nu \leq 190 \text{ GeV}$ and $E_{J/\psi} \geq 80 \text{ GeV}$, we find $R(\text{Sn}/\text{C}) = 0.82 \pm 0.06$ which is compatible with the FNAL value. A meaningful comparison with the EMC result [23] is not possible, since their resolution in z and p_T^2 did not allow a complete subtraction of the coherent contribution. They found $R(\text{Fe}/(\text{H} + \text{D})) = 1.45 \pm 0.12(\text{stat.}) \pm 0.22(\text{syst.})$ which lies between our values for $R_{\text{in}}(\text{Sn}/\text{C})$ and $R_{\text{coh}}(\text{Sn}/\text{C})$.

5. Summary and conclusions

We have measured the ratio of cross sections for J/ψ production in deep inelastic muon scattering for tin and carbon. Our ability to separate the different kinematic regions permits the various results from previous experiments to be reconciled. The ratio $R(\text{Sn}/\text{C})$ of cross sections per nucleon is significantly larger than unity for coherent processes in which the nucleus emerges intact from the interaction. For quasielastic J/ψ production the cross section per nucleon for tin is significantly lower than that for carbon. For inelastic J/ψ production we found $R_{\text{in}}(\text{Sn}/\text{C}) = 1.13 \pm 0.08$. This can be interpreted in the framework of the Colour Singlet model as an enhancement of the gluon distribution of tin with respect to carbon.

We wish to thank the technical staff of CERN and of the participating institutes for their invaluable contributions to the experiment. We are also grateful to N.N. Nikolaev and T. Sloan for fruitful discussions.

References

- [1] EMC Collab., J.J. Aubert et al., Phys. Lett. B123 (1983) 275
- [2] SLAC-E139 Collab., R.G. Arnold et al., Phys. Rev. Lett. 52 (1984) 727; SLAC-PUB-3257 (1983); BCDMS Collab., G. Bari et al., Phys. Lett. B163 (1985) 282; BCDMS Collab., A.C. Benvenuti et al., Phys. Lett. B189 (1987) 483; EMC-NA2' Collab., J. Ashman et al., Phys. Lett. B202 (1988) 603; EMC-NA28 Collab., M. Arneodo et al., Nucl. Phys. B333 (1990) 1; NMC Collab., P. Amaudruz et al., Z. Phys. C51 (1991) 387
- [3] T. Sloan, G. Smadja and R. Voss, Phys. Rep. 162 (1988) 45
- [4] L. Frankfurt and M. Strikman, Phys. Rep. 160 (1988) 235; R.J.M. Covolan and E. Predazzi, in Problems of fundamental modern physics, Ed. R. Cherubini, P. Dalpiaz and B. Minetti (World Scientific, Singapore, 1991) p. 85
- [5] E.L. Berger and D. Jones, Phys. Rev. D23 (1981) 1521
- [6] EMC Collab., N. Dyce, Ph.D. thesis, Lancaster University (1988)
- [7] NMC Collab., D. Allasia et al., Phys. Lett. B258 (1991) 493
- [8] NMC Collab., M. de Jong, Ph.D. thesis, Free University of Amsterdam (1991)
- [9] NMC, C. Mariotti, Nucl. Phys. A532 (1991) 437c
- [10] NMC Collab., D. Allasia et al., CERN/SPSC 85-18; NMC Collab., F. Zetsche, Ph.D. thesis, University of Heidelberg (1990), in German
- [11] Review of Particle Properties, Phys. Lett. B239 (1990) 1
- [12] R. Barate et al., Z. Phys. C33 (1987) 505
- [13] T.H. Bauer et al., Rev. Mod. Phys. 50 (1978) 261; E. Paul, Nucl. Phys. A446 (1985) 203
- [14] T. de Forest and J.D. Walecka, Adv. in Phys. 15 (1966) 1
- [15] I. Sick, Nucl. Phys. A218 (1974) 509; I. Sick, Phys. Lett. B116 (1982) 212
- [16] A.D. Martin, C.-K. Ng and W.J. Stirling, Phys. Lett. B191 (1987) 200
- [17] F.E. Close, J. Qiu and R.G. Roberts, Phys. Rev. D40 (1989) 2820

- [18] U. Sukhatme, G. Wilk and K.E. Lassila, UICHEP-TH/90-10, (1990)
- [19] L.L. Frankfurt, M.I. Strikman and S. Liuti, *Phys. Rev. Lett.* 65 (1990) 1725
- [20] R.L. Anderson et al., *Phys. Rev. Lett.* 38 (1977) 263
- [21] M.D. Sokoloff et al., *Phys. Rev. Lett.* 57 (1986) 3003
- [22] EMC Collab., J.J. Aubert et al., *Phys. Lett.* B152 (1985) 433
- [23] EMC Collab., J.J. Aubert et al., *Nucl. Phys.* B213 (1983) 1